MOLECULAR AND CELLULAR BIOLOGY, Jan. 2001, p. 636–643 Vol. 21, No. 2
0270-7306/01/$04.00+0 DOI: 10.1128/MCB.21.2.636–643.2001
Copyright © 2001, American Society for Microbiology. All Rights Reserved.

Mutation and Analysis of *Dan*, the Founding Member of the Dan Family of Transforming Growth Factor β Antagonists

MARC S. DIONNE, WILLIAM C. SKARNES, AND RICHARD M. HARLAND*

Division of Genetics and Development, Department of Molecular and Cell Biology, University of California, Berkeley, California 94720

Received 13 October 2000/Accepted 18 October 2000

The Dan family of transforming growth factor β antagonists is a large, evolutionarily conserved family of proteins. Little is known about either the specificity of these antagonists or the biological roles of these proteins. We have characterized *Dan*, the founding member of this family, with regard to both its biochemical specificity and its biological roles. Although DAN is not an efficient antagonist of BMP-2/4 class signals, we found that DAN was able to interact with GDF-5 in a frog embryo assay, suggesting that DAN may regulate signaling by the GDF-5/6/7 class of BMPs in vivo. Intriguingly, in developing neurons, *Dan* mRNA was localized to axons, suggesting a potential role for the DAN protein in axonal outgrowth or guidance. Mice lacking *Dan* activity were generated by gene targeting and displayed subtle, background-dependent defects.

Bone morphogenetic proteins (BMPs) were first isolated biochemically as activities that could induce ectopic bone formation in rat soft tissues. When the active proteins were purified and sequenced and the genes encoding them were cloned, they were found to be homologous to the *Drosophila* gene *decapentaplegic* (*dpp*), a member of the transforming growth factor β (TGF-β) superfamily of secreted signals (25, 36, 39). *dpp* and the two other *Drosophila* BMP family members, *screw* and *glass-bottomed boat*/*60A*, play roles in a wide variety of developmental processes, including the establishment of initial dorsal-ventral polarity in the *Drosophila* ectoderm and development of various imaginal disc-derived structures (8). This family of proteins has undergone dramatic evolutionary expansion: vertebrate genomes contain 20 or more BMPs (23). Loss-of-function mutants in the vertebrate BMPs display a tremendous variety of defects, and BMP overexpression can cause a wide variety of developmental defects (11).

Vertebrate genomes also encode many proteins that block signaling by TGF-β family members; these are generally called TGF-β or BMP antagonists. The largest group of these antagonists is the DAN family of proteins (13, 26, 35). There are at least seven DAN family members in the mouse, including *DAN* (differential screening-selected gene aberrative in neuroblastoma) itself, *mCer1*, *gremlin*, *PRDC*, and several genes that have only been identified as expressed sequence tags (3, 13, 22). This family is marked by a shared cysteine-rich domain and by a resemblance to the mucins, a family of secreted factors found in mucus (13, 26). It is unclear whether the similarity to mucin is functionally meaningful. DAN family members are believed to act by binding BMPs within the extracellular space (13, 27).

Dan was originally cloned as a transcript downregulated in *src*-transformed rat fibroblasts (24). DAN has been shown to be able to bind BMP-2 in vitro; however, interaction between DAN and any specific TGF-β under physiological conditions remains to be demonstrated (13). Although DAN can bind BMP-2 at high concentrations, the early phenotype of *DAN* overexpression in the frog embryo is distinct from those of other BMP antagonists, and hence argues against the BMP-2/4 and BMP-7 classes of BMPs as physiological ligands for DAN (13, 32).

In order to understand better the in vivo roles of DAN, we designed bioassays for BMP blockade within the *Xenopus* embryo, examined *Dan* expression in the mouse, and generated mice that lacked DAN function. In this way, we have shown that DAN may bind GDF-5 in vivo, that *Dan* mRNA is localized in many developing axon tracts, and that *Dan* mutant mice have only subtle defects.

MATERIALS AND METHODS

Library screening and generation of targeting constructs. IMAGE clone 441413, encoding mouse DAN, was obtained from Research Genetics; an 873-bp *Pst*I-*Pvu*II fragment from this clone was used to screen a mouse 129/Sv genomic library by standard methods (28). Multiple clones were isolated and restriction mapped to verify that rearrangements had not occurred in the library. One lambda clone, designated λ10, was used to generate the regions of homology used in both targeting vectors.

(i) pDANλ10F/R. For construction of pDANλ10F/R, a 12-kb phage insert which contained the entire DAN cDNA was cloned as follows. λ10 was cut with *Not*I and cloned into *Not*I-cut, phosphatase-treated pBluescript SK− (Stratagene). The F orientation indicates that the DAN gene reads from the *Sac*I end to the *Kpn*I end of the polylinker, and the R orientation indicates the reverse.

(ii) pLoxP2.1. In order to simplify construction of the targeting constructs, two tandem *loxP* sites were inserted into the pBluescript polylinker. Two oligonucleotides were constructed: loxP1 (GAT CAT AAC TTC GTA TAA TGT ATG CTA TAC GAA GTT ATA AGC TTA GAT CT) and loxP2 (AGA TCT AAG CTT ATA ACT TCG TAT AGC ATA CAT TAT ACG AAG TTA T). These oligonucleotides were annealed by heating to 90°C and then allowing them to slowly return to room temperature. The resulting double-stranded fragment was phosphorylated with T4 polynucleotide kinase, resulting in a linker with the structure 5′ GATC end-*loxP* site-*Hin*dIII-*Bgl*II-blunt end. This linker was blunted with T4 DNA polymerase, cut with *Hin*dIII, and inserted between the *Eco*RV and *Hin*dIII sites in pBluescript SK−, resulting in pLoxP2. The (uncut) linker was then cloned between the *Bam*HI and *Sma*I sites in pLoxP2, resulting in pLoxP2.1. The selected clone was sequenced to confirm that there were no mutations in the *loxP* sites; a base had been lost in the first ligation, resulting in the regeneration of the *Eco*RV site (and the loss of a planned *Bcl*I site).

* Corresponding author. Mailing address: 401 Barker Hall, Department of Molecular and Cell Biology, University of California, Berkeley, CA 94720-3202. Phone: (510) 643-6003. Fax: (510) 643-1729. E-mail: harland@socrates.berkeley.edu.

(iii) pdko1. Plasmid pdko.1 carried a targeting construct which removed the final exon of the *Dan* gene. A β-actin-neo-SV40pA cassette was cut from pBKNPA (W.C. Skarnes, unpublished observations) with *Bam*HI and *Bg1*II; the resulting fragment was inserted into the *Bg1*II site in pLoxP2.1, resulting in the plasmid pLoxβneoF. pDANλ10F was cut with *Spe*I, blunted, and then cut with *Kpn*I; the resulting fragment was inserted into pLoxβneoF between the *Kpn*I and blunted *Cla*I sites, resulting in the plasmid pLoxβneo3′. Finally, pdko1 was generated by cutting pLoxβneo3′ with *Spe*I and inserting the 4-kb *XbaI* fragment from pDANλ10F.

(iv) pdko3. Plasmid pdko3 carried a targeting construct which inserted an internal ribosome entry site (IRES)-placental alkaline phosphatase (PLAP) cassette into the *Dan* gene. pBKNPA was cut with *Xba*I, blunted, and then cut with *Eco*RI; this was inserted into *Pst*I (blunt)-*Eco*RI-cut pLoxP2.1. The resulting plasmid was cut with *Eco*RI and *Eco*RV, and the PGK-neo-BPA cassette was inserted as an *Eco*RI-*Xho*I (blunt) fragment from pPGKneoTK (19). The IRES-PLAP cassette was cut from pGTO-IP (W.C. Skarnes, unpublished observations) with *Xba*I and inserted into the *Spe*I site, resulting in the plasmid pIP1. Two oligonucleotides were constructed: bglsph3 (GTG ATG ACA CCG GTG GAT GTC GTC GAC ATG) and bglsph4 (TCG ACG ACA TCC ACC GGT GTC ATC ACC TG). These oligonucleotides were annealed as described for pLoxP2.1, resulting in a linker with the structure 3′ CTG end-*Sgr*AI-*Sal*I-3′ CATG end. A 6.3-kb *Eco*RI-*Xho*I fragment was cut from pDANλ10F and inserted into pBluescript SK−. This plasmid was then cut with *Sph*I and *Bg1*I, and the *Bg1*I-*Sph*I linker above was inserted. The resulting plasmid was cut with *Cla*I and *Not*I, and the 3.2-kb *Not*I-*Cla*I fragment from pdko1 was inserted, resulting in pHRV9. pIP1 was cut with *Not*I and partly filled with G's, resulting in a 3′ GG overhang; this was then cut with *Sal*I, liberating the IRES-PLAP-PGK-neo-BPA cassette. This fragment was ligated into pHRV9, which had been cut with *Sgr*AI, partly filled with C's and then cut with *Sal*I, producing pdko3.

Generation of *Dan* mutant mice; genotyping and mouse husbandry. pdko1 and pdko3 were grown as multiple 100-ml cultures in *Escherichia coli*. DNA was purified from bacterial cultures by using Qiagen Maxiprep kits. Each construct was linearized (pdko1 with *Sac*I; pdko3 with *Xho*I) and electroporated into E14 ES cells as previously described (31), except that 75 μg of DNA and 5×10^7 cells were used for each electroporation. Selection was carried out in 175 μg of G418 per ml (Gibco). ES cell lines were analyzed by Southern blotting with a 5′ flanking probe (the *Ase*I-*Sac*I fragment shown in Fig. 3A) and a probe specific for neomycin phosphotransferase, as previously described (12). With the dko1 vector, 310 lines were analyzed, of which 8 carried the desired mutant allele; with the PLAP vector, 300 lines were analyzed, of which 1 carried the desired mutant allele.

Two dko1 lines (101 and 237) and the PLAP line (K93) were injected into C57BL/6J blastocysts. All three lines produced mutant progeny. Chimeras were crossed onto C57BL/6J (Jackson) and 129S6SvEv (Taconic) females; lines were maintained by backcross onto wild-type females of the appropriate inbred strain. Animals were genotyped either by Southern blotting or by PCR as previously described (12). Genomic DNA for Southern blotting was cut with *Ase*I and either *Bam*HI (for Dan^{PLAP}) or *Eco*RV (for Dan^{dko1}). All PCR genotyping was done with Platinum *Taq* (Gibco). The cycling conditions were 2 min at 95°C and 35 cycles of 30 s at 95°C, 30 s at 60°C, and 1 min at 72°C. The following primers were used: for allele dko1, dan5 (CAC TCG GGT CCA GGG GAG ATG G), dan8 (CTG GAC CCT TTA GGA AAG TAG C), and neo5 (CAC ACC TCC CCC TGA ACC TG), resulting in a 361-bp wild-type product and a 280-bp mutant product, and for the PLAP allele, danap1-2 (ACA ATG CTT TGG GTC CTG GTG G), danap2-5 (TTC CTC TAG TTC TAG AGC GGC C), and danap 3-2 (CTG AAG CAT TGT CCT AGG CAC GC), resulting in a 300-bp wild-type product and a 170-bp mutant product. *Noggin* mice were genotyped by PCR as previously described (19).

***Xenopus* embryo assays.** *Xenopus* embryos were staged, cultured and injected as previously described (18). Ventral marginal zone explants were cut at stage 10.25 and cultured in Sater's modified blastocoel buffer until sibling embryos had reached stage 20 for analysis of muscle actin gene expression (30). Reverse transcription-PCR (RT-PCR) analysis was carried out as previously described (38).

Skeletal preparations. Skeletal preparations were performed as previously described (17).

Whole-mount in situ hybridization. In situ hybridization was carried out essentially as described previously (37) with the following changes. All stages previous to probe hybridization were carried out on ice, and 0.1 M NaP (1 M NaP is 0.5 M Na_2HPO_4, with pH adjusted to 7.5 with H_3PO_4) was substituted for phosphate-buffered saline (PBS); mouse powder was not used; and antibody incubation and postantibody washes were carried out in a mixture of 1× MAB (1× MAB is 100 mM maleic acid plus 150 mM NaCl adjusted to pH 7.5 with NaOH), 0.1% bovine serum albumin (BSA) and 2% BM blocking reagent (Boehringer-Mannheim). Embryos at e12.5 or later were usually cut into pieces after initial fixation to aid reagent penetration.

PLAP staining. Heads from embryos to be stained for alkaline phosphatase activity were fixed overnight in 4% paraformaldehyde–1× HeBS (10× HeBS is 82 g of NaCl per liter 59.5 g of HEPES acid per liter 1.05 g of Na_2HPO_4 pH per liter, with pH adjusted to 7 with NaOH) at 4°C. Roughly 18 h later, embryos were rinsed multiple times and then stored at 4°C in 1× HeBS for as long as several weeks.

For sectioning, embryos or heads were dried thoroughly with a Kimwipe and embedded in 5% low-melt agarose (Gibco)–1× HeBS. One hundred-micrometer sections were cut on a vibratome, allowed to dry at room temperature, and then immersed in 1× HeBS. Endogenous phosphatases were inactivated by heating to 65°C for 45 min. The slides were cooled to room temperature, and the HeBS was replaced with AP buffer (100 mM Tris [pH 9.5], 100 mM NaCl, 50 mM $MgCl_2$). After 3 min, the AP buffer was replaced with AP buffer supplemented with 175 μg of BCIP (5-bromo-4chloro-3-indolylphosphate) and 337.5 μg of nitroblue tetrazolium per ml. Sections were then allowed to react in the dark for 2 h at 37°C.

Once sections were stained, slides were rinsed in 1× PBS or 1× HeBS, allowed to sit for a few minutes, and then taken through 25, 50, and 75% ethanol (EtOH) in water to 100% EtOH). The 100% EtOH was changed once, and then slides were transferred to Hemo-De (Fisher). Hemo-De was changed twice, and then slides were mounted with Permount (Fisher).

Fluorescent antibody staining of sections. Embryos were dissected on ice and fixed for 2 to 3 h in 4% paraformaldehyde–0.1 M sodium phosphate buffer (pH 7.5) at 4°C, rinsed twice in 0.1 M NaP buffer, and then transferred to 0.1 M NaP buffer–30% sucrose at 4°C and allowed to equilibrate for 24 h. At the end of this period, they were embedded in TBS tissue freezing medium (Fisher) and sectioned on a cryotome at a 20-μm thickness.

Slides were then washed three times for 5 min each in 1× PBS, which was then changed for PHT (PBS plus 1% heat-inactivated goat serum, 0.1% Triton X-100). After 30 min in PHT, slides were removed from the bath and placed upside-down on 200-μl drops of primary antibody mix (1:200 dilution of affinity-purified rabbit polyclonal anti-MATH1 antibody in anti-MASH1 antibody supernatant) that had been placed on Parafilm (American National Can Company). These were then incubated overnight at 4°C, washed three times in 1× PBS for 10 min each, and then placed upside-down as before on drops containing 1:150 Texas red-conjugated goat-anti-rabbit immunoglobulin G(IgG) and 1:200 Fluorescein isothiocyanate-conjugated goat-anti-mouse IgG in 1× PBS (secondary antibodies were from Jackson Immunoresearch); secondary antibodies were allowed to bind for at least 2 h at room temperature. Slides were then once again washed three times for 10 min each in 1× PBS and mounted with Vectashield (Vector Research).

RESULTS AND DISCUSSION

DAN bioassays. We wished to understand DAN's physiological role better by identifying TGF-βs that could interact with DAN in a biological context. The *Xenopus* embryo is an excellent system for analyzing interactions between TGF-βs and their antagonists, since the embryo provides distinct readouts for different kinds of TGF-β activities. Several BMPs are expressed in the *Xenopus* embryo at this stage of development (4, 9, 10, 14). Overexpression of BMP-2/4-class or BMP-7-class signals in the early mesoderm induces ventral fates, while inhibitors of these signals (such as *Noggin*, *Xnr3*, *Chordin*, or *Follistatin*) induce dorsal fates (6). *Dan* can mimic the dorsalization caused by these inhibitors in mesodermal explants, although inefficiently (13, 32). This suggested to us that, while DAN was apparently able to antagonize BMP-4 or BMP-7 when provided in sufficient excess, the BMP-2/4 and BMP-7 classes of signals were unlikely to be physiological targets for DAN. We examined the GDF-5/6/7 class as potential DAN targets, because this group of BMPs is the next most closely related to the other two classes at a sequence level (16, 34).

The interaction between DAN and GDF-5 can be assayed indirectly, by testing whether GDF-5 can block the dorsalizing

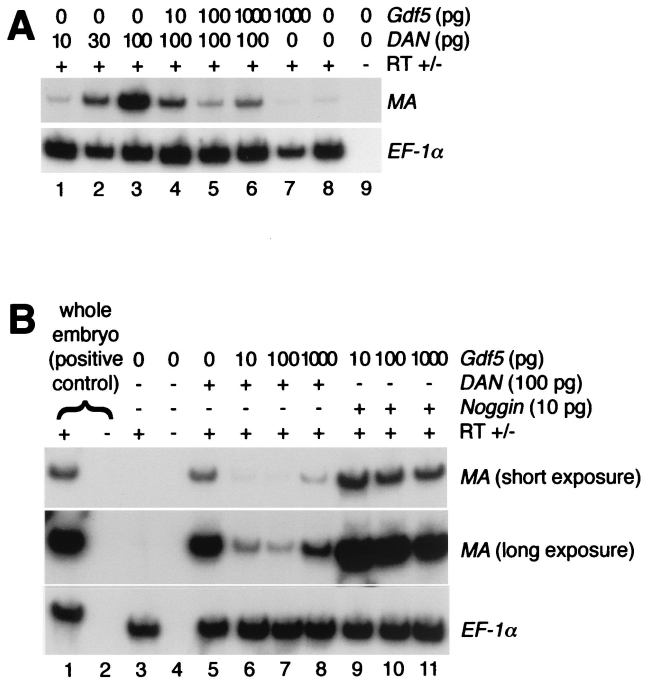

FIG. 1. GDF-5 blocks DAN activity. *Xenopus* embryos were injected on the ventral side at the four-cell stage with the doses of *Dan* and *Gdf5* mRNA shown. Embryos were cultured until the beginning of gastrulation, and then the ventral marginal zones were explanted and cultured until sibling embryos had reached stage 20, when they were lysed and assayed by RT-PCR for expression of muscle-specific cardiac actin, a marker of paraxial mesoderm. (A) In lanes 1 to 3, increasing doses of *Dan* induced increasing expression of muscle-specific cardiac actin (MA); in lanes 4 and 5, increasing doses of *Gdf5* blocked this induction with increasing efficiency. Intriguingly, extremely high doses of *Gdf5* blocked *DAN* less efficiently (compare lanes 5 and 6); this result was seen in three separate experiments and remains unexplained. As expected, *Gdf5* alone did not induce MA above background levels, even at high doses (lanes 7 and 8), and when the RT was omitted, no background was visible. (B) In addition to *Dan-Gdf5* coinjections, *Gdf5* was also coexpressed with *Noggin*. In addition to repeating the result shown above, this experiment also showed that *Gdf5* was unable to efficiently counter *Noggin*-induced dorsalization, as seen in lanes 9 to 11.

effects of DAN: in essence, by asking if GDF-5 is able to compete efficiently with the other BMPs in the early embryo to bind DAN. We used this assay because, in our hands, GDF-5 caused no obvious phenotype in the *Xenopus* embryo even when expressed at very high levels (data not shown). If GDF-5 is a physiological DAN ligand, it should compete with endogenous BMPs to bind *Dan* and hence efficiently prevent *Dan*-induced mesoderm dorsalization. We found that even small doses of GDF-5 were sufficient to reproducibly antagonize DAN-mediated dorsalization (Fig. 1A). Moreover, GDF-5 was unable to significantly reverse Noggin-induced dorsalization, even when *Gdf5* mRNA was present in 100-fold excess over *Noggin* mRNA (Fig. 1B). This suggests that the reversal of *Dan*-induced dorsalization was a result of GDF-5 binding directly to DAN rather than a result of it signaling through BMP receptors. Although these experiments do not show direct binding of GDF-5 by DAN, they suggest that in the *Xenopus* embryo, DAN may interact with GDF-5 with a higher affinity than with the endogenous members of the BMP-2/4 and BMP-7 classes. Noggin has previously been shown to interact directly with GDF-5 in vitro (21); our results suggest that Noggin's affinity for GDF-5 in vivo may be significantly lower than that for BMP-4.

***Dan* mRNA localization in axons.** Expression of *Dan* in the early mouse embryo has been described previously (26, 32). However, in examining *Dan* expression by in situ hybridization, we made the surprising observation that *Dan* mRNA was localized to many axon tracts in the developing mouse fetus (Fig. 2). This staining was visible as early as e11.5; embryos processed in parallel with a variety of other probes did not show similar staining. This staining appeared to be axonal and not specific to glia or other support cells, since the only glia which are present at this time and place are white-matter astrocytes, which display little resemblance to the cells stained (15, 29). Not all axon tracts were stained, in keeping with the restricted

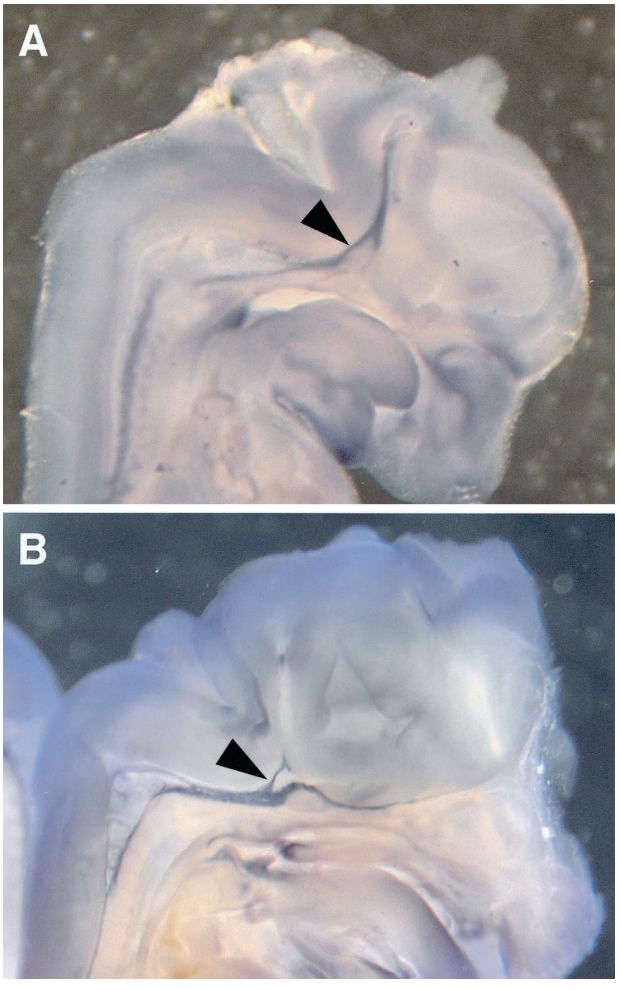

FIG. 2. *Dan* mRNA was found in axon tracts. Embryos were split in half sagittally and subjected to whole-mount in situ hybridization. (A) An e12.5 embryo. (B) An e14.5 embryo. In both cases, DAN mRNA was strongly localized in many of the descending projections from the forebrain and midbrain (arrowheads). The arrowhead in panel B points out a specific tract in which the cell bodies and the projections could be distinguished; based on its location and the developmental stage of the embryo, this may be the medullar projection from the arcuate nucleus of the hypothalamus.

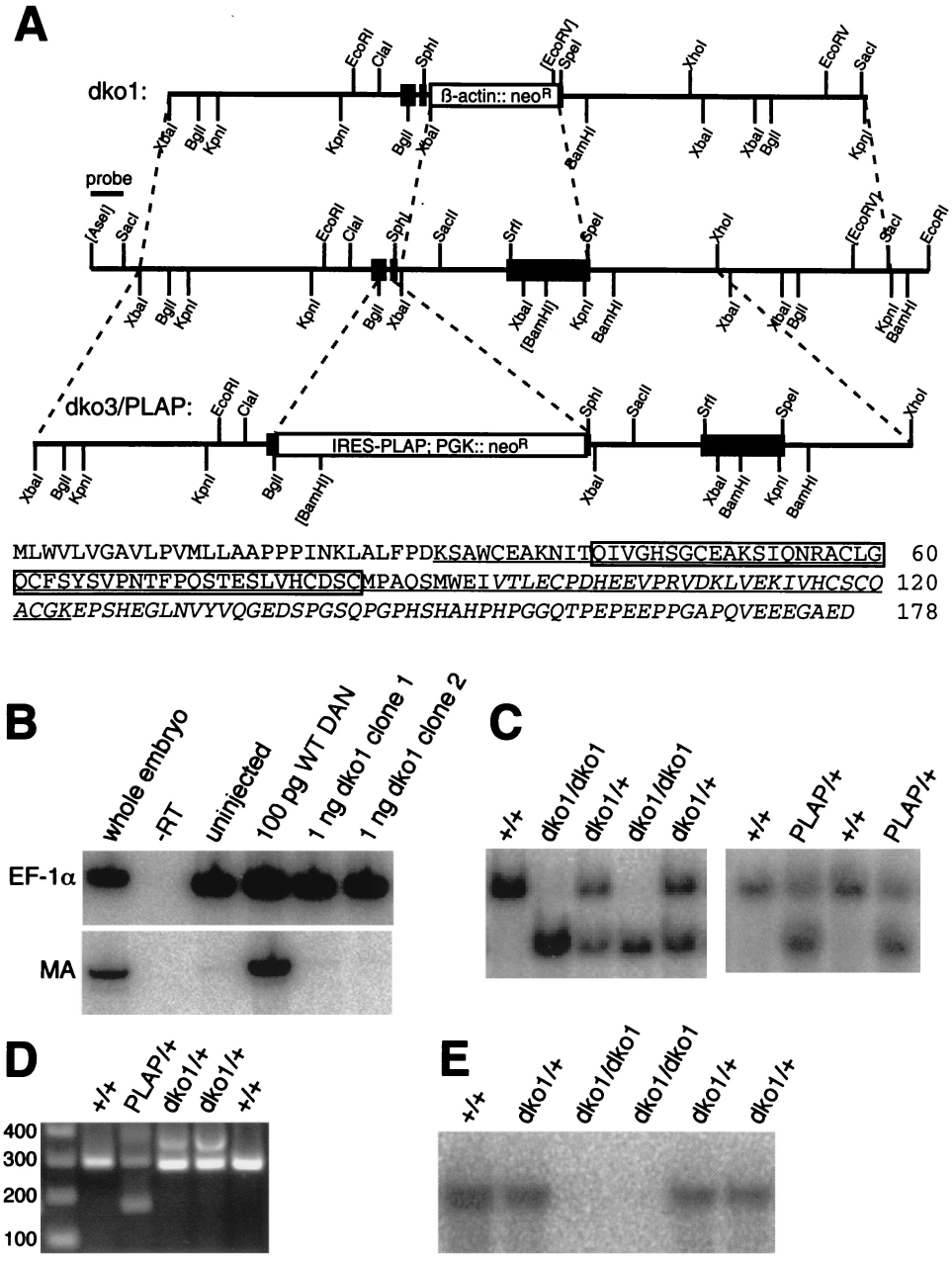

FIG. 3. Targeting of the *Dan* locus. (A) Map of the wild-type *Dan* locus and the two knockout constructs. All genes in this figure are transcribed from left to right; all exons of the *Dan* gene are shown. The top construct is for Dan^{dkol}, which removed intron II and exon III; the bottom construct is for Dan^{PLAP}, which removed parts of exons I and II and intron I. Bracketed restriction sites are those used for genotyping by Southern blotting, with the probe shown (between the *Ase*I and *Sac*I sites at the left end of the DAN genomic fragment). Below is shown the amino acid sequence of the DAN protein. The underlined region is the conserved cysteine-rich domain shared by DAN family members; the boxed region was removed in Dan^{PLAP}, and the region in italic was removed in Dan^{dkol}. (B) RT-PCR analysis showing that the portions of the *Dan* protein retained in Dan^{dkol} mice had no detectable residual activity in a frog embryo dorsalization assay. Ventral marginal zones from embryos injected with 100 pg of wild-type *Dan* mRNA expressed high levels of muscle-specific cardiac actin (MA), a marker of paraxial mesoderm, while those from uninjected embryos or embryos injected with 1 ng of Dan^{dkol} mRNA displayed no muscle actin expression. (Wild-type *DAN* will robustly induce muscle actin at doses ranging from 50 pg to several nanograms.) EF-1α is a loading control; the lane labeled "−RT" is a control sample treated without reverse transcriptase. (C) Genotyping of Dan^{dkol} and Dan^{PLAP} mice by Southern blotting. The left-hand blot was made from tail DNA cut with *Eco*RV and *Ase*I; the right-hand blot was made from tail DNA cut with *Bam*HI and *Ase*I. (D) Genotyping of Dan^{dkol} and Dan^{PLAP} mice by PCR. The left two lanes (aside from the ladder) were analyzed for Dan^{PLAP}; the right three lanes were analyzed for Dan^{dkol}. (E) Southern blot of genomic DNA cut with *Ase*I and *Eco*RV and probed with a 500-bp *Bgl*II fragment from exon III of *Dan*. As predicted, hybridization was lost in DNA from Dan^{dkol} mice. This blot had been probed previously with the genotyping probe to confirm the genotypes of these mice and to verify that all lanes were loaded with similar amounts of DNA.

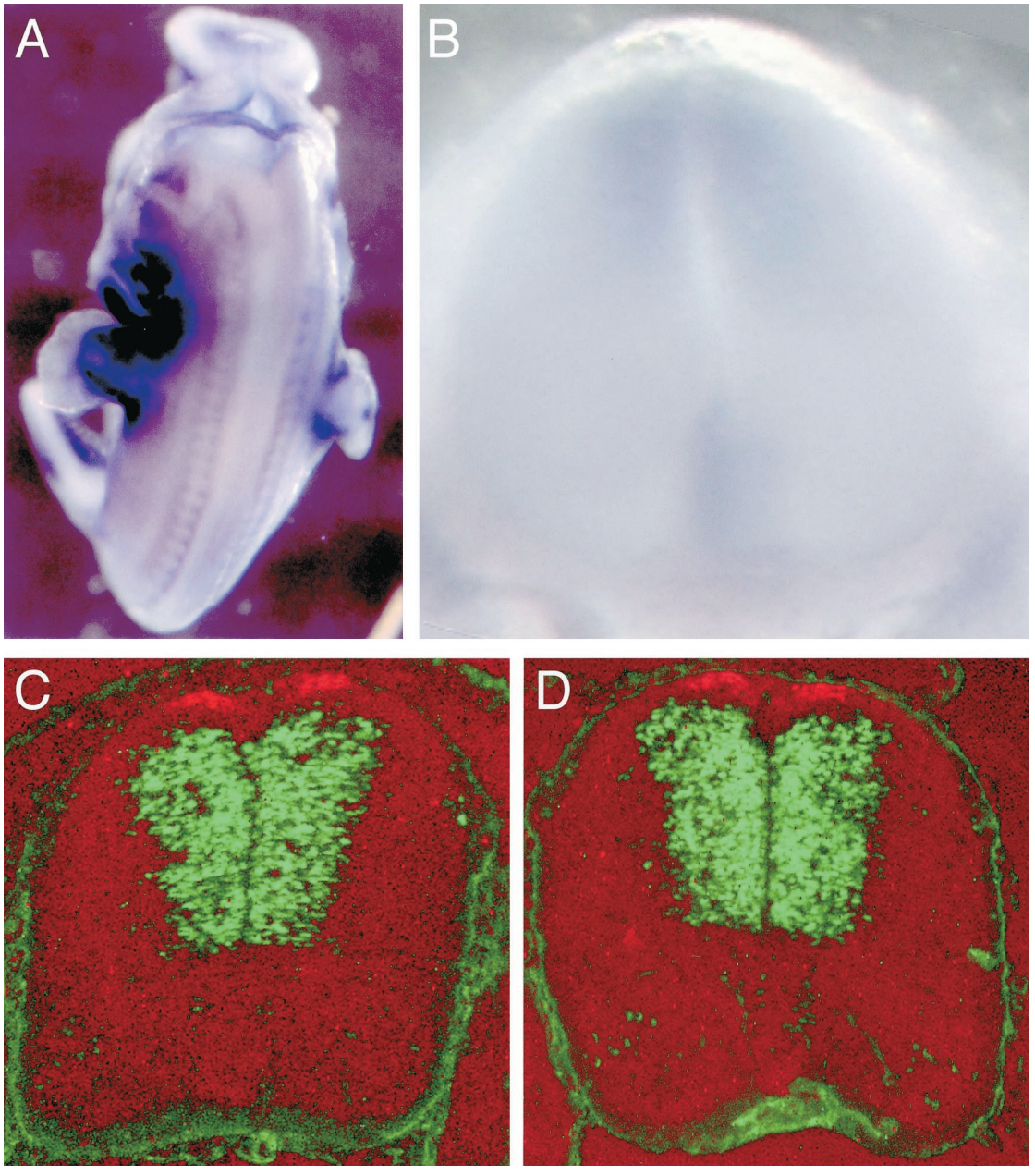

FIG. 4. *Dan*$^{dkol/dkol}$ animals showed no defect in patterning of the dorsal spinal cord. (A and B) *Dan* expression in the spinal cord at e11.5 (A) and e12.5 (B). (C and D) Transverse sections through the spinal cord at the level of the forelimb of a wild-type mouse (C) and a *Dan* mutant at e12.5 (D). Red indicates *MATH1* expression, which marks dorsal interneuron precursors; green indicates *MASH1* expression, which marks a variety of neuronal precursor types in the dorsomedial part of the ventricular zone.

Dan expression seen in the developing brain. In some cases (including the animal shown), it was possible to trace the staining back along the axons all the way to the cell bodies; in these cases, the cell bodies appeared no more strongly stained than the axon. Such localization has previously been suggested to be characteristic of mRNAs encoding proteins which are required in distal portions of the developing axons (33).

Generation of *Dan* mutant mice. In order to address biological roles for DAN, we generated mice carrying two mutant alleles of the *Dan* gene. *Dan* consists of three exons; the *Dan*^{dkol} allele replaces nearly all of the third exon of *Dan* with a β-actin::Neo^{r} cassette, while the *Dan*^{PLAP} allele replaces much of the first two exons and the entire first intron with an IRES—PLAP; PGK::Neo^{r} cassette (Fig. 3A). We chose to make mice carrying the PLAP marker because our observation that *Dan* mRNA was localized to axons led us to hypothesize that the mutant mice might exhibit some defect in axon guidance that would be most easily analyzed by being able to specifically stain DAN-expressing axons.

Both alleles delete significant portions of the DAN family conserved region (Fig. 3A). Moreover, *Dan*^{PLAP} separates the remaining C-terminal portion of the protein from the N-ter-

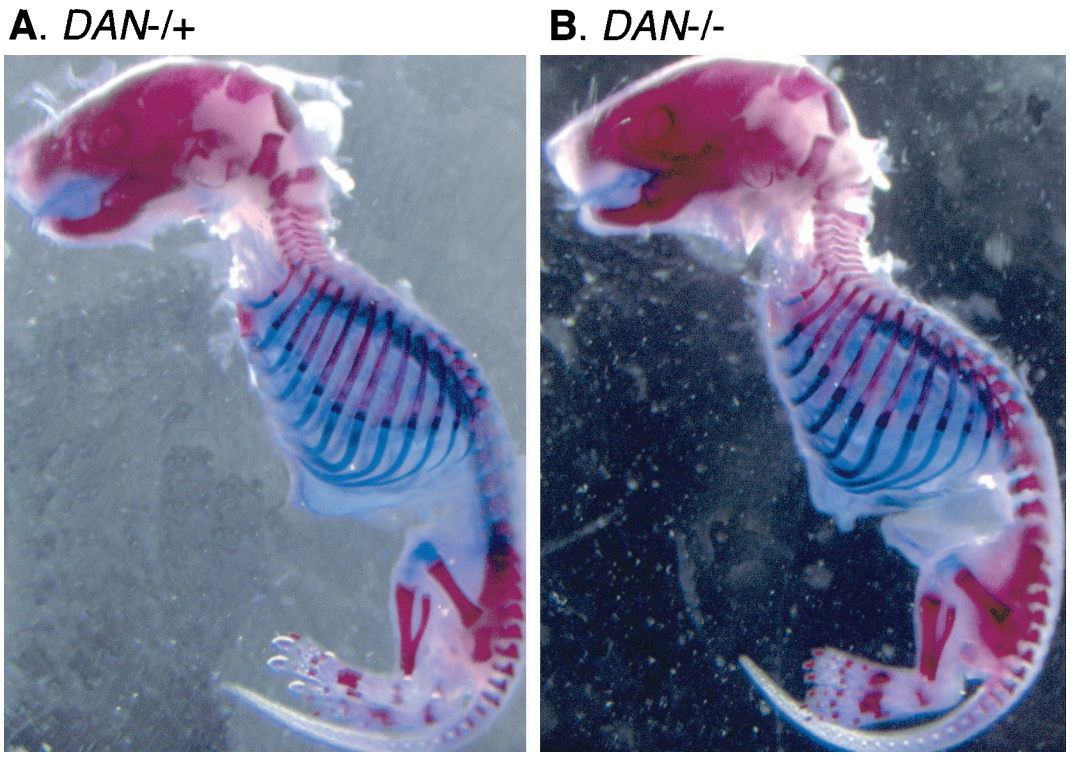

FIG. 5. No gross skeletal defects were apparent in newborn $Dan^{dkol/dkol}$ animals. Blue staining indicates cartilage, while red is bone. (A) A *Dan* heterozygote. (B) A homozygous mutant, both on the 129S6SvEv inbred background.

minal secretory signal. In order to verify that Dan^{dkol} had little remaining activity, we injected mRNA encoding the predicted mutant protein into *Xenopus* embryos. No morphological defects resulted from this overexpression in the whole embryo (data not shown). Moreover, this mutant form had lost the ability to induce muscle actin expression in explanted ventral marginal zones, even when expressed at levels 10-fold higher than those required for robust induction by the wild-type protein (Fig. 3B), suggesting that the mutant allele was either a very strong hypomorph or a null allele.

Mutant mice were genotyped by Southern blotting with a 5′ probe (Fig. 3C), using a Neo^r probe (data not shown), or by PCR (Fig. 3D). Dan^{dkol} DNA was also blotted with a probe made to the deleted portion of the gene; no hybridization was visible with this probe in homozygous mutant mice (Fig. 3E).

Mice homozygous for either *Dan* mutant allele were viable, fertile, and displayed no obvious morphological or behavioral abnormalities, whether they were crossed onto a C57BL/6J background or onto a 129S6SvEv background. Dan^{dkol} mutant animals were born in the expected numbers from crosses of heterozygotes (for the C57BL/6J background, of 371 animals, 96 were wild type, 179 were heterozygous, and 96 were homozygous; for the 129S6SvEv background, of 183 animals, 46 were wild type, 91 were heterozygous, and 46 were homozygous).

Characterization of *Dan* mutants. Early *Dan* expression (from e8 to e11.5) has previously been described; at these stages, *Dan* is expressed in head mesoderm, somites, facial structures, and limbs (26, 32). No defects were apparent in any of these structures in mutant mice (data not shown).

BMP family members have been found to be able to regulate dorsal-ventral patterning of the spinal cord and hindbrain, and we had observed diffuse *Dan* expression in the developing neural tube at e11.5 and e12.5 (Fig. 4A and B) (1, 16). Accordingly, we examined dorsal-ventral patterning of these structures in the *Dan* mutants. No alterations were observed in expression of *Math-1* or *Mash-1* in the spinal cord (Fig. 4C and D) or at the rhombic lip (data not shown) of *Dan* mutant mice.

Because of the localization we had previously observed of *Dan* mRNA in axons and because BMPs have previously been characterized as axon-guidance cues both in mammals and in *Caenorhabditis elegans* (2, 5), we examined mice carrying the Dan^{PLAP} allele for defects in axon tracts that were positive for PLAP activity at e14.5. No abnormalities were seen in these tracts, suggesting that *Dan* is not required for proper axonal pathfinding in the cells in which it is expressed.

Recent data suggest that *Noggin* is required for correct generation of limb tendons (C. Tabin, personal communication). *Dan* mRNA is expressed in the ventral limb tendons at e12.5 (data not shown). We assayed *Dan* mutant embryos for perturbations in expression of the tendon marker *scleraxis* at e12.5. No defects were apparent (data not shown). Additionally, no defects were apparent in visual examination of the ventral limb tendons of adult *Dan* mutant mice (data not shown).

Because DAN can antagonize BMP-class signals, we examined *Dan* mutant mice for skeletal defects (13, 32). No defects were apparent in *Dan* mutant pups on either genetic background (Fig. 5). We also examined mice that lacked *Dan* and were heterozygous for *Noggin*. On the 129S6SvEv background,

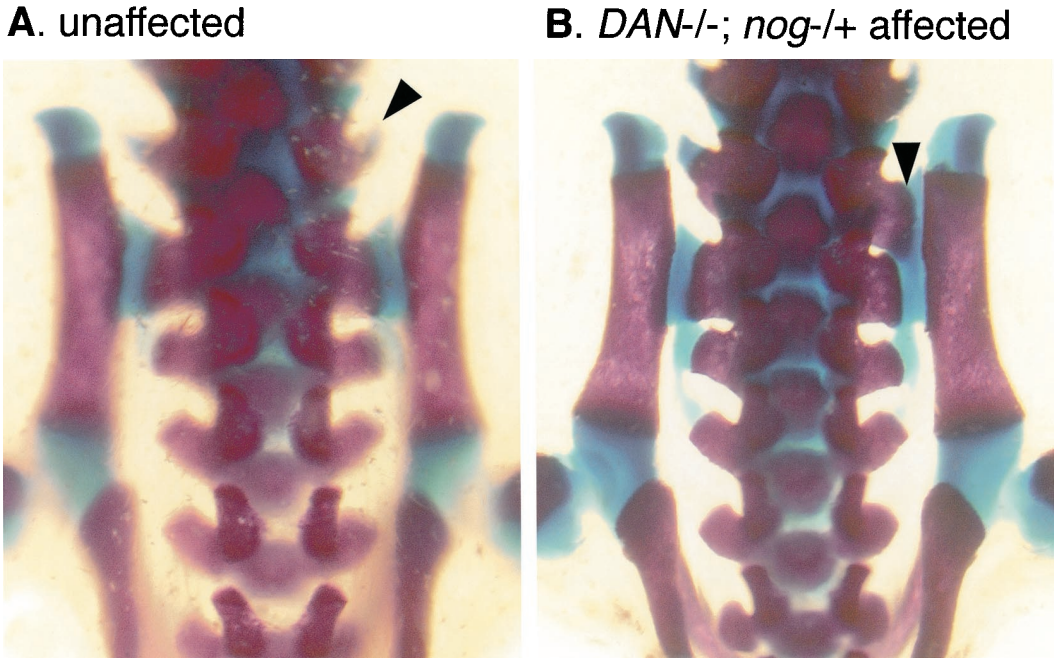

FIG. 6. The skeletal defect in $Dan^{dkol/dkol}$ $Nog^{-/+}$ animals. The left panel shows the sacral vertebrae of an unaffected animal, while the right panel shows an animal in which the right-hand side of the last lumbar vertebra was affected. In each panel, the right-hand side of the last lumbar vertebra is indicated with an arrowhead.

28% ($n = 7$) of these animals displayed an apparent transformation of the right-hand side of the last lumbar vertebra to a sacral fate (Fig. 6). No *Dan*-heterozygote or *Dan-Noggin* transheterozygote animals ($n = 15$) displayed this defect. This defect is particularly interesting in the context of recent work showing that *Gdf11* acts as a global regulator of anterior-posterior pattern in the skeleton (20). *Gdf11* mutant mice display posterior-to-anterior transformations throughout the axial skeleton, including extra ribs and posteriorward shifts of specific vertebral landmarks and the hindlimbs and posteriorward shifts in expression of a number of *Hox* genes (20). DAN and Noggin may be involved in region-specific regulation of the BMP or GDF signals in order to properly regulate anteroposterior identity in the posterior lumbar region. However, specific blocking of GDF-11 by DAN or Noggin seems unlikely: DAN was unable to block the activity of GDF-8, a close relative of GDF-11 (data not shown), and others have found that Noggin is unable to block GDF-11 signaling (7). A more likely possibility is that DAN and Noggin may be responsible for antagonism of other TGF-β family members in the region which would otherwise mis-specify the local regional identity. Another possibility is that the apparent lumbar-to-sacral conversion is not a true homeotic transformation, but rather an alteration in the morphology of the last lumbar vertebra so that it resembles a sacral vertebra.

We have presented data which suggest that DAN may be an antagonist of GDF-5/6/7 signals in vivo. *Dan* mRNA was localized within developing axons. This suggested a potential role for DAN in rendering the extending axons resistant to environmental GDF-5/6/7 signals; however, when we generated *Dan* mutant mice, we found no apparent defects in proper extension or pathfinding by the expressing axons. The *Dan* mutant mice were viable and fertile, with no obvious abnormalities. These mice displayed no defects in proper dorsal-ventral patterning of the spinal cord or in skeletal development. However, mice lacking *Dan* and heterozygous for *Noggin* displayed, at low penetrance, an apparent homeotic transformation of the last lumbar vertebra to a sacral fate.

ACKNOWLEDGMENTS

We thank Kathy Pinson for blastocyst injections; Lisa Brunet for assistance with mouse husbandry; Mustafa Khokha for tendon dissections; Karen Liu, Tim Grammer, and John "Six-guns" Wallingford for comments on the manuscript; and all the members of the Harland and Skarnes laboratories for many helpful discussions. The anti-MATH1 antibody was a gift of A. Helms and J. Johnson, the anti-MASH1 antibody was a gift of D. J. Anderson, and the murine genomic library was a gift of C. Stewart.

This work was funded by NIH grants to W.C.S. and R.M.H.

REFERENCES

1. **Alder, J., K. J. Lee, T. M. Jessell, and M. E. Hatten.** 1999. Generation of cerebellar granule neurons in vivo by transplantation of BMP-treated neural progenitor cells. Nat. Neurosci. **2:**535–540.
2. **Augsburger, A., A. Schuchardt, S. Hoskins, J. Dodd, and S. Butler.** 1999. BMPs as mediators of roof plate repulsion of commissural neurons. Neuron **24:**127–141.
3. **Bouwmeester, T., S. Kim, Y. Sasai, B. Lu, and E. M. De Robertis.** 1996. Cerberus is a head-inducing secreted factor expressed in the anterior endoderm of Spemann's organizer. Nature **382:**595–601.
4. **Chang, C., and A. Hemmati-Brivanlou.** 1999. Xenopus GDF6, a new antagonist of noggin and a partner of BMPs. Development **126:**3347–3357.
5. **Colavita, A., S. Krishna, H. Zheng, R. W. Padgett, and J. G. Culotti.** 1998. Pioneer axon guidance by UNC-129, a C. elegans TGF-beta. Science **281:**706–709.
6. **Dale, L., and C. M. Jones.** 1999. BMP signalling in early Xenopus development. Bioessays **21:**751–760.
7. **Gamer, L. W., N. M. Wolfman, A. J. Celeste, G. Hattersley, R. Hewick, and V. Rosen.** 1999. A novel BMP expressed in developing mouse limb, spinal cord, and tail bud is a potent mesoderm inducer in Xenopus embryos. Dev. Biol. **208:**222–232.

8. **Gelbart, W. M.** 1989. The *decapentaplegic* gene: a TGF-beta homologue controlling pattern formation in *Drosophila*. Development **107**(Suppl.)**:**65–74.
9. **Hawley, S. H., K. Wunnenberg-Stapleton, C. Hashimoto, M. N. Laurent, T. Watabe, B. W. Blumberg, and K. W. Cho.** 1995. Disruption of BMP signals in embryonic Xenopus ectoderm leads to direct neural induction. Genes Dev. **9:**2923–2935.
10. **Hemmati-Brivanlou, A., and G. H. Thomsen.** 1995. Ventral mesodermal patterning in Xenopus embryos: expression patterns and activities of BMP-2 and BMP-4. Dev. Genet. **17:**78–89.
11. **Hogan, B. L.** 1996. Bone morphogenetic proteins: multifunctional regulators of vertebrate development. Genes Dev. **10:**1580–1594.
12. **Hogan, B. L. M., R. Beddington, F. Costantini, and E. Lacy.** 1994. Manipulating the mouse embryo: a laboratory manual, 2nd ed. Cold Spring Harbor Laboratory Press, Plainview, N.Y.
13. **Hsu, D. R., A. N. Economides, X. Wang, P. M. Eimon, and R. M. Harland.** 1998. The Xenopus dorsalizing factor Gremlin identifies a novel family of secreted proteins that antagonize BMP activities. Mol. Cell **1:**673–683.
14. **Jones, C. M., K. M. Lyons, P. M. Lapan, C. V. Wright, and B. L. Hogan.** 1992. DVR-4 (bone morphogenetic protein-4) as a posterior-ventralizing factor in Xenopus mesoderm induction. Development **115:**639–647.
15. **Kettenmann, H., and B. R. Ransom (ed.).** 1995. Neuroglia. Oxford University Press, New York, N.Y.
16. **Lee, K. J., M. Mendelsohn, and T. M. Jessell.** 1998. Neuronal patterning by BMPs: a requirement for GDF7 in the generation of a discrete class of commissural interneurons in the mouse spinal cord. Genes Dev. **12:**3394–3407.
17. **Lufkin, T., M. Mark, C. P. Hart, P. Dollé, M. LeMeur, and P. Chambon.** 1992. Homeotic transformation of the occipital bones of the skull by ectopic expression of a homeobox gene. Nature **359:**835–841.
18. **Mariani, F. V., and R. M. Harland.** 1998. XBF-2 is a transcriptional repressor that converts ectoderm into neural tissue. Development **125:**5019–5031.
19. **McMahon, J. A., S. Takada, L. B. Zimmerman, C. M. Fan, R. M. Harland, and A. P. McMahon.** 1998. Noggin-mediated antagonism of BMP signaling is required for growth and patterning of the neural tube and somite. Genes Dev. **12:**1438–1452.
20. **McPherron, A. C., A. M. Lawler, and S. J. Lee.** 1999. Regulation of anterior/posterior patterning of the axial skeleton by growth/differentiation factor 11. Nat. Genet. **22:**260–264.
21. **Merino, R., D. Macias, Y. Ganan, A. N. Economides, X. Wang, Q. Wu, N. Stahl, K. T. Sampath, P. Varona, and J. M. Hurle.** 1999. Expression and function of Gdf-5 during digit skeletogenesis in the embryonic chick leg bud. Dev. Biol. **206:**33–45.
22. **Minabe-Saegusa, C., H. Saegusa, M. Tsukahara, and S. Noguchi.** 1998. Sequence and expression of a novel mouse gene PRDC (protein related to DAN and cerberus) identified by a gene trap approach. Dev. Growth Differ. **40:**343–353.
23. **Neuhaus, H., V. Rosen, and R. S. Thies.** 1999. Heart specific expression of mouse BMP-10 a novel member of the TGF-beta superfamily. Mech. Dev. **80:**181–184.
24. **Ozaki, T., and S. Sakiyama.** 1993. Molecular cloning and characterization of a cDNA showing negative regulation in v-*src*-transformed 3Y1 rat fibroblasts. Proc. Natl. Acad. Sci. USA **90:**2593–2597.
25. **Padgett, R. W., R. D. St. Johnston, and W. M. Gelbart.** 1987. The *decapentaplegic* gene complex of *Drosophila* encodes a protein homologous to the transforming growth factor-beta gene family. Nature **325:**81–84.
26. **Pearce, J. J., G. Penny, and J. Rossant.** 1999. A mouse cerberus/Dan-related gene family. Dev. Biol. **209:**98–110.
27. **Piccolo, S., E. Agius, L. Leyns, S. Bhattacharyya, H. Grunz, T. Bouwmeester, and E. M. De Robertis.** 1999. The head inducer Cerberus is a multifunctional antagonist of Nodal, BMP and Wnt signals. Nature **397:**707–710.
28. **Sambrook, J., E. F. Fritsch, and T. Maniatis.** 1989. Molecular cloning: a laboratory manual, 2nd ed. Cold Spring Harbor Laboratory Press, Cold Spring Harbor, N.Y.
29. **Silver, J., M. A. Edwards, and P. Levitt.** 1993. Immunocytochemical demonstration of early appearing astroglial structures that form boundaries and pathways along axon tracts in the fetal brain. J. Comp. Neurol. **328:**415–436.
30. **Sive, H. L., R. M. Grainger, and R. M. Harland.** 2000. Early development of Xenopus laevis: a laboratory manual. Cold Spring Harbor Laboratory Press, Cold Spring Harbor, N.Y.
31. **Skarnes, W. C., J. E. Moss, S. M. Hurtley, and R. S. Beddington.** 1995. Capturing genes encoding membrane and secreted proteins important for mouse development. Proc. Natl. Acad. Sci. USA **92:**6592–6596.
32. **Stanley, E., C. Biben, S. Kotecha, L. Fabri, S. Tajbakhsh, C. C. Wang, T. Hatzistavrou, B. Roberts, C. Drinkwater, M. Lah, M. Buckingham, D. Hilton, A. Nash, T. Mohun, and R. P. Harvey.** 1998. DAN is a secreted glycoprotein related to Xenopus cerberus. Mech. Dev. **77:**173–184.
33. **Steward, O.** 1997. mRNA localization in neurons: a multipurpose mechanism? Neuron **18:**9–12.
34. **Storm, E. E., T. V. Huynh, N. G. Copeland, N. A. Jenkins, D. M. Kingsley, and S. J. Lee.** 1994. Limb alterations in brachypodism mice due to mutations in a new member of the TGF beta-superfamily. Nature **368:**639–643.
35. **Topol, L. Z., M. Marx, D. Laugier, N. N. Bogdanova, N. V. Boubnov, P. A. Clausen, G. Calothy, and D. G. Blair.** 1997. Identification of *drm*, a novel gene whose expression is suppressed in transformed cells and which can inhibit growth of normal but not transformed cells in culture. Mol. Cell. Biol. **17:**4801–4810.
36. **Wang, E. A., V. Rosen, P. Cordes, R. M. Hewick, M.-J. Kriz, D. P. Luxenberg, B. S. Sibley, and J. M. Wozney.** 1988. Purification and characterization of novel bone-inducing factors. Proc. Natl. Acad. Sci. USA **85:**9484–9488.
37. **Wilkinson, D. G.** 1992. Whole mount in situ hybridization of vertebrate embryos, p. 75–83. *In* D. G. Wilkinson (ed.), In situ hybridization: a practical approach. IRL Press, Oxford, United Kingdom.
38. **Wilson, P. A., and D. A. Melton.** 1994. Mesodermal patterning by an inducer gradient depends on secodary cell-cell communication. Curr. Biol. **4:**676–686.
39. **Wozney, J. M., V. Rosen, A. J. Celeste, L. M. Mitsock, M. J. Whitters, R. W. Kriz, R. M. Hewick, and E. A. Wang.** 1988. Novel regulators of bone formation: molecular clones and activities. Science **242:**1528–1534.